Optimizing Rapid Diffusion Kurtosis Imaging Sequences for Clinical Translation in Radiation Oncology

Marek Obajtek[1,3], Ekaterina Tchistiakova[1,2,3], Shima Y. Tari[3], Ali Golestani[1,2,3]

[1]Department of Physics and Astronomy, University of Calgary, Calgary, AB
[2]Department of Oncology, University of Calgary, Calgary, AB
[3]Arthur J.E. Child Comprehensive Cancer Centre, Cancer Care Alberta, Calgary, AB

Cancer Care Alberta

UNIVERSITY OF CALGARY

Introduction

- Quantitative diffusion MRI parameters are a growing area of clinical interest
- Apparent diffusivity (D) was found to be a good predictor of patient outcomes in radiation therapy[1]
- Apparent kurtosis (K) paired with the diffusion coefficient have been shown to correlate well with grading of cancerous tumour tissue[1]
- Methods such as diffusion kurtosis imaging[2] (DKI), which measure more than one quantitative diffusion parameter, are often too long for incorporation in clinical workflows[3]
- **Aim:** Study and time-optimize DKI sequences using an ablation study[4] with a greedy search algorithm[5]

Can this time-optimization open the door to clinical translation of sequences like DKI?

Methods

The NIST/QIBA diffusion phantom[6] (CaliberMRI, Boulder, CO, USA) and a pineapple were each imaged at 14 non-zero b-values (30-3000 s/mm^2) and b = 0 s/mm^2. 8 images were acquired for each of 15 b-values and 6 isotropic gradient directions. These were processed to create a set of diffusion weighted images (DWIs) for parameter fitting. The following stochastic greedy search[5] was performed as outlined:

1. Randomly test-remove (ablate) one image for each b-value, re-process and re-fit parameter maps, and compare to the baseline using the Hotelling's T^2 statistic[7].
2. Once this has been done for all b-values, permanently remove 1 image used in averaging for the b-value with the lowest T^2. The next iteration, the remaining images will be randomly reshuffled from the total set to avoid bias.
3. Iteratively repeat points 1. and 2. until two images remain.
4. To improve the search for minima, also test-remove entire b-values in each iteration (premature b-value removal).

The optimal image subset was determined from an elbow in the T^2 error plot.

DKI fitting was performed using PyTorch's Adam optimizer[8,9], with physical parameter bounds enforced using the softplus and/or sigmoid functions.

Discussion

- Sawtooth oscillations are not yet fully understood
  - Expectation of full b-value removal corresponding to error drops only explains a small fraction of cases, and only when the removal is premature
- Width of T^2 histogram characterizes the reliability of the optimization and chosen optimum
  - Pineapple images have lower SNR than phantom ones, i.e. worse scan repeatability
  - With greater histogram widths, the quality of the optimization steps is called into question
- Kurtosis was the main contributor to T^2 increase
  - Image reduction has minor effects on diffusivity
  - In phantom fits, kurtosis errors were dependent on polyvinylpyrrolidone (PVP) concentrations of vials[6]
  - Pineapple kurtosis error map had high heterogeneity
- Rician noise flooring[10] was responsible for kurtosis overestimations in water and low PVP vials

Results

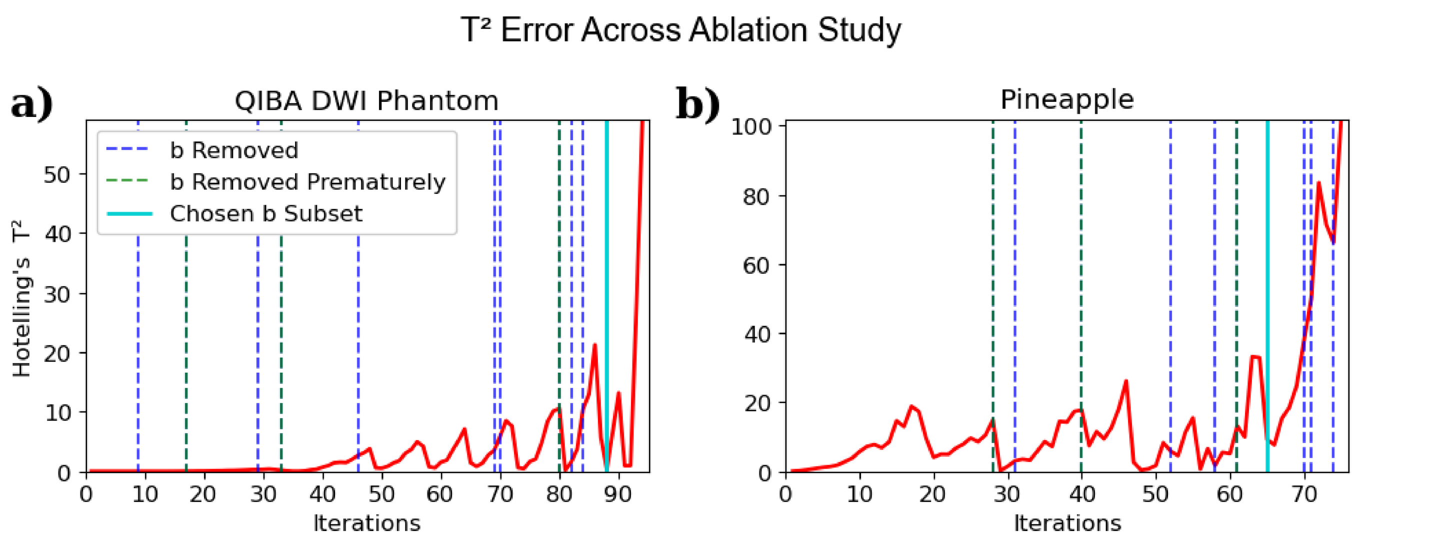

Figure 1. *Error plot of T^2 across the optimization for (a) the QIBA DWI phantom and (b) pineapple. Dashed lines indicate iterations after which an entire b-value was removed, where green ones represent premature removals. The turquoise lines indicate the chosen reduced image subsets.*

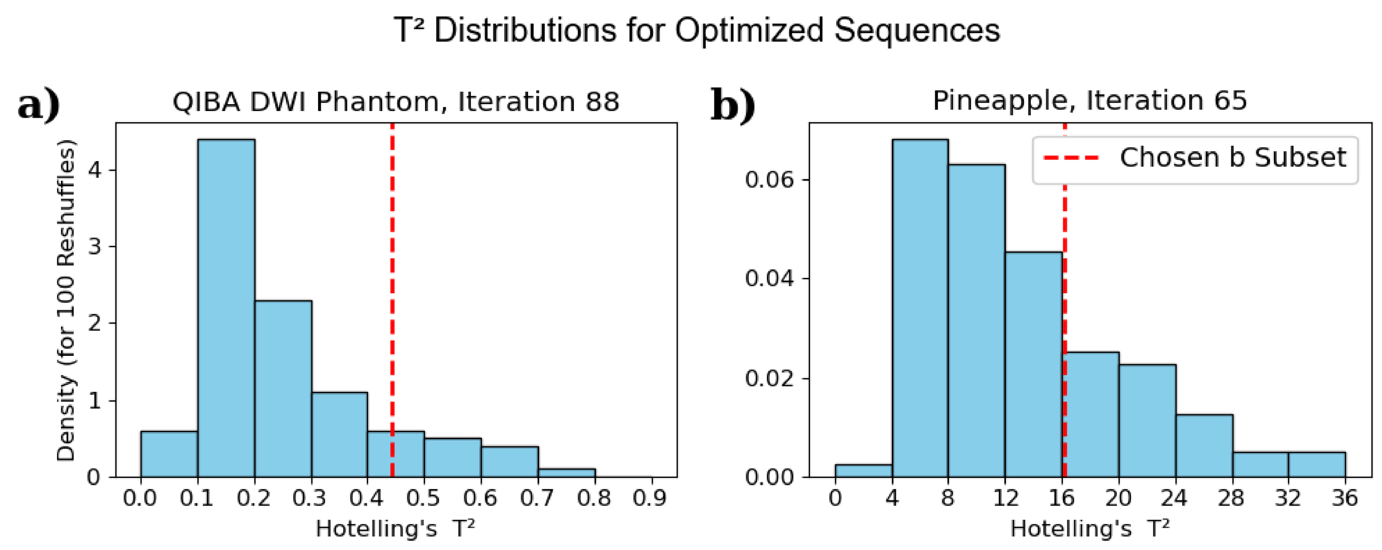

Figure 2. *T^2 histograms generated from 100 random reshuffled image subsets for (a) the QIBA DWI phantom and (b) pineapple, chosen from iterations 88 and 65 in the respective optimizations. The red dashed lines represent the T^2 values of the fits used in Figures 3c and 3d.*

- Error plots exhibited sawtooth oscillations (Figure 1)
  - Sudden T^2 drops are largely independent of full b-value removals
  - Premature b-value removals are more likely to be associated with a sudden drop in T^2
- Selected optimized subsets
  - Phantom: $T^2 = 0.282$, 28/120 images
  - Pineapple: $T^2 = 9.24$, 41/120 images
- Subsets re-run with resampling 100 times (Figure 2)
  - Phantom: T^2 distribution in range [0, 0.8]
  - Pineapple: T^2 distribution in range [0, 36]
- Chose to look at fits in mid-high range of T^2 values (Figure 3; Phantom T^2 : 0.443, Pineapple T^2 : 16.2)
  - Percent error in maps more heterogenous for kurtosis

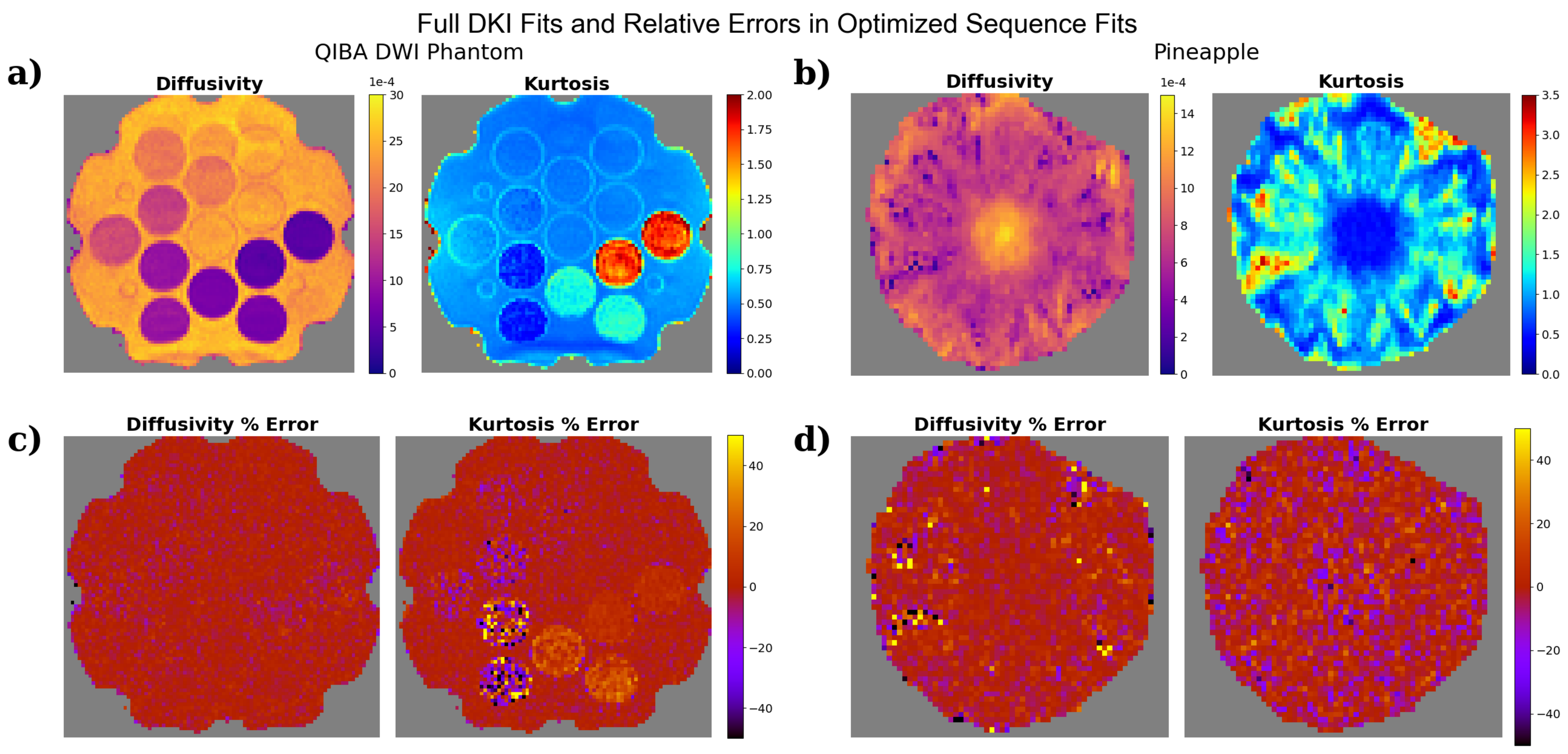

Figure 3. *Fits of mean diffusivity and mean kurtosis for (a) the QIBA DWI phantom and (b) pineapple, using the full image sets. (c) and (d) represent the respective percent errors of the optimized sequence fits relative to (a) and (b).*

Conclusion

- A novel stochastic greedy algorithm was designed and was able to reduce the number of images required for accurate DKI fits
- Fitting and optimization results are highly dependent on target parameter distributions and scan data quality
- Success of the work, expanded in scope and application, will enable the clinical translation of quantitative diffusion MRI towards cancer care workflows

We successfully developed an ablation algorithm for the time-optimization of DKI.

Future work will focus on 1) Rician noise floor removal[10], 2) optimization of gradient directions, 3) human scans and expanding the signal model to include perfusion parameters[11], as well as 4) justified initial b-value selection[12].

Contact Information

marek.obajtek@cancercarealberta.ca

References (cont.)

Please scan for the full list of references

References

1. Granata V, Fusco R, Belli A, et al. Diffusion weighted imaging and diffusion kurtosis imaging in abdominal oncological setting: why and when. Infect Agent Cancer. 2022;17(1):25.
2. Jensen JH, Helpern JA, Ramani A, et al. Diffusional kurtosis imaging: the quantification of non-gaussian water diffusion by means of magnetic resonance imaging. Magn Reson Med. 2005;53(6):1432–1440.
3. Palumbo P, Martinese A, Antenucci MR, et al. Diffusion kurtosis imaging and standard diffusion imaging in the magnetic resonance imaging assessment of prostate cancer. Gland Surg. 2023;12(12):1806–1822.